Available online at www.sciencedirect.com
SCIENCE DIRECT®
New Astronomy Reviews 47 (2003) 1091–1096
New Astronomy Reviews
www.elsevier.com/locate/newastrev

Polarization comparison between on-axis and off-axis dual reflector telescopes: Zemax and Grasp8 simulations

Huan T. Tran

Miller Institute, University of California, Berkeley, CA 94720-7300, USA

Abstract

The cross-polarization performance for an off-axis dual reflector telescope is shown to be equivalent to an on-axis telescope when used for a large-format focal plane array. The need for low sidelobes forces the on-axis designs to high curvature, which in turn leads to high cross-polarization at the edge of the field. A scheme for correcting instrumental-polarization is presented, as well as a full design for a polarization-pure optical system capable of supporting a 1000-element focal plane array.

1. Introduction

The recent interest measuring the Gravitational B-mode signature in the polarization of the Cosmic Microwave background has forced experimenters to revisit basic design considerations. Not only is a new level of sensitivity required, but also a more detailed understanding of systematic errors is needed to measure signals that may be three or more orders of magnitude smaller than the current level of detectability.

The need for higher sensitivity motivates the use of large-format arrays, which in turns mandates the use of telescopes with a large field of view (FOV). There are generally three separate anisotropy spectra; the temperature, the E-mode, and the B-mode. The amplitude of these different anisotropies are different from each other by orders of magnitude, so a design with a high degree of dynamic range is required. A telescope with polarization purity will prevent the temperature and E-mode power spectra from leaking into the B-mode spectrum.

One lesson to be learned from successful temperature anisotropy experiments is that for non-interferometric scanning beam-type measurements, a clean, well defined beam with low sidelobes and high efficiency is desirable. This is generally only achievable with unblocked apertures.

Another requirement for a successful gravitational B-mode experiment is that it have high resolution. Although the gravity wave signal imprints itself at degree-scale angular resolution, it is necessary to measure the anisotropy at much higher resolution to remove contaminants. The

E-mail address: huantran@cosmology.berkeley.edu (H.T. Tran).

1387-6473/$ - see front matter
doi:10.1016/j.newar.2003.09.035

most notable contaminant is the gravitational lensing signal, which imprints itself at smaller ($\sim 10'$) scales (Hu and Okamoto, 2002; Kesden et al., 2003; Knox and Song, 2002).

In addition to cosmological contaminants, there are instrumental sources of contamination. The topic of these proceedings is how well telescope design can mitigate these offsets. In general, if the offsets can be well characterized, some level of removal is possible. So stability of the contaminant is more important than the magnitude. It is, however, difficult to estimate the stability of the offsets, so the best strategy is to make the offsets as small as possible.

The desire for unobstructed and large apertures leads naturally to off-axis reflector designs. It can also be shown that a Gregorian with a Mizuguchi–Dragone type correction has a large enough FOV (Hanany and Marrone, 2002). There is a concern, however, that off-axis designs will have excessive polarized contamination. The cylindrical symmetry of on-axis systems is sometimes assumed to lead to a high degree of polarization purity. We will use Zemax, a raytracer and Grasp8, a physical optics simulation tool to evaluate these issues. Specifically, the cross-polarized beams will be compared between on- and off-axis systems. Additionally, a strategy for correcting instrumental-polarization will be presented. Finally, a full design for a polarization pure optical system will be presented, including reimaging optics.

2. Instrumental contaminants

In an effort to clarify the effects of different types of polarized contamination, two broad categories of leakage can be identified, cross-polarization and instrumental-polarization. Both sources of leakage can be dealt with in different manners, as will be discussed in Sections 5 and 6. Both forms of contamination also effect polarization measurements differently, and the difference can be derived with some simple formalism.

The polarization properties of devices can be represented in terms of Jones matrices. It is customary, however, to characterize astronomical polarization in terms of the Stokes vectors. It is usually easier to intuit the Jones matrix for a given device, so a procedure for converting from one format to the other is necessary. A simple procedure for doing so is outlined in O'Dell (2001) and will be summarized here.

The procedure borrows heavily from quantum mechanics. The critical notion is the distinction between when the radiation is merely modified and when it is detected. Detection is represented by the scalar quantity formed from the *state vector*, $|E\rangle$ (a Jones vector), and the matrix operation, $\mathbf{O}$

$$\langle \mathbf{O} \rangle = \langle E|\mathbf{O}|E\rangle. \tag{1}$$

In the case of perfect Stokes parameter detectors, the $\mathbf{O}$ matrices can be written as

$$\mathbf{I} = \begin{pmatrix} 1 & 0 \\ 0 & 1 \end{pmatrix}, \quad \mathbf{Q} = \begin{pmatrix} 1 & 0 \\ 0 & -1 \end{pmatrix}, \quad \mathbf{U} = \begin{pmatrix} 0 & 1 \\ 1 & 0 \end{pmatrix}, \quad \mathbf{V} = \begin{pmatrix} 0 & -\mathrm{i} \\ \mathrm{i} & 0 \end{pmatrix}. \tag{2}$$

2.1. Cross-polarization

One type of instrumental contamination, known as cross-polarization, cross-couples orthogonal Jones vectors. The Jones matrix for cross-polarization can be written as

$$\mathbf{C} = \begin{pmatrix} \sqrt{1-\epsilon} & -\sqrt{\epsilon}\,\mathrm{e}^{\mathrm{i}\psi} \\ +\sqrt{\epsilon}\,\mathrm{e}^{-\mathrm{i}\psi} & \sqrt{1-\epsilon} \end{pmatrix}, \tag{3}$$

where the particular form of $\mathbf{C}$ comes from Heiles et al. (2001) and was chosen to make it unitary. The parameter ϵ is a measure of the degree of cross-coupling, and is usually small. Note that $\mathbf{C}$ is very close to the rotation operator,

$$\mathbf{R} = \begin{pmatrix} \cos\phi & \sin\phi \\ -\sin\phi & \cos\phi \end{pmatrix}, \tag{4}$$

with the exception of an additional possible phase shift, ψ. To calculate the effect of cross-polarization on the measurement of Q, the following construction can be evaluated:

$$\langle Q' \rangle = \langle E|\mathbf{C}^{\dagger}\mathbf{Q}\mathbf{C}|E\rangle. \tag{5}$$

The new operator, $\mathbf{C}^{\dagger}\mathbf{Q}\mathbf{C}$, gives a more realistic representation of a Q measuring device. This expression can be decomposed into the operators given in Eq. (2):

$$\mathbf{C}^{\dagger}\mathbf{Q}\mathbf{C} = (1-2\epsilon)\mathbf{Q} - 2\sqrt{(1-\epsilon)\epsilon}\cos\psi\mathbf{U} - 2\sqrt{(1-\epsilon)\epsilon}\sin\psi\mathbf{V}. \quad (6)$$

This equation makes it clear that the action of cross-polarization is to mix Q, U, and V. Furthermore, if $\psi = 0$, that is, if the cross-polarization is a pure rotation, then it only mixes Q and U. Mixing between Q and U leads to leakage from E-modes to B-modes. Since the power in E-modes is likely to be at least an order of magnitude larger than B-modes, this can be a problem even if the leakage is small. Typically, telescope optics will have $\epsilon \approx 1\%$.

2.2. Instrumental-polarization

Instrumental-polarization is caused by oblique reflection from surfaces with finite conductivity. It can be divided into two classes; emission and absorption. The emissive portion varies only with temperature and will likely be stable enough to subtract (Johnson, 2003). Absorption is more problematic in that it has the potential to contaminate the B-mode signal with signal from the temperature anisotropies. The preferential absorption of one polarization by the telescope optics leads to a spurious polarized signal when observing an unpolarized source.

The Jones matrix for the absorbing instrumental-polarization may be written as

$$\mathbf{P} = \begin{pmatrix} g_1 & 0 \\ 0 & g_2 e^{i\psi} \end{pmatrix}, \quad (7)$$

where the differential absorption appears as a difference in the gains, g_1 and g_2. Again, a possible phase shift ψ appears between the two axis. Note that there is an assumed orientation in writing this equation, namely that the instrumental-polarization axis lies along axis defined by the matrix basis.

As with the cross-polarization, the effect of instrumental-polarization on $\mathbf{Q}$ can be shown to be

$$\mathbf{P}^{\dagger}\mathbf{Q}\mathbf{P} = \frac{g_1^2 - g_2^2}{2}\mathbf{I} + \frac{g_1^2 + g_2^2}{2}\mathbf{Q}. \quad (8)$$

For $\mathbf{U}$, the corresponding equation is

$$\mathbf{P}^{\dagger}\mathbf{U}\mathbf{P} = g_1 g_2 \cos\psi\mathbf{U} - g_1 g_2 \sin\psi\mathbf{V}. \quad (9)$$

One interesting thing to note is that Q and U do not mix. This only happens because the axis of the instrumental-polarization were assumed to be along the basis in which Q and U are defined. In other words, if Q and U are measured in the basis defined by the instrumental-polarization, Q and U will not mix. Perhaps more problematically, however, I will leak into Q, which means that the temperature map will leak into the Q map. Salvation may lie in the fact that if the basis is chosen properly, I does not leak into U, so in principle, there may be a way to estimate how much of the temperature map is leaking into the polarization maps if there is one clean channel.

3. Optical comparisons

To compare on- and off-axis designs, two roughly equivalent systems were chosen. An existing off-axis system, the Viper telescope operating at the South Pole,[1] was chosen as a representative off-axis millimeter telescope. The 2-mirror Viper Telescope has a 2 m primary and a overall $F/\# = 5.2$. The primary and secondary are figured as an aplanatic Gregorian, also known as a Ritchey–Cretian. The on-axis system was also chosen to be a Ritchey–Cretian with identical aperture and $F/\#$.

There is, however, one degree of freedom with the Ritchey–Cretian, which is the secondary size. As the secondary gets bigger, the diffraction limited FOV increases but the sidelobe level also increases. To quantify this statement, both a raytracing and physical optics simulation were performed on a $F/5.2$ 2 m Ritchey–Cretian. For the physical optics simulation, a feed horn with a gaussian edge taper of −12 dB was used. In Fig. 1, the variation of both the diffraction-limited FOV and the sidelobe level with secondary size is shown. There is a clear trade-off between sidelobe level and FOV. The desire for low sidelobe level

[1] http://cmbr.phys.cmu.edu/vip.html.

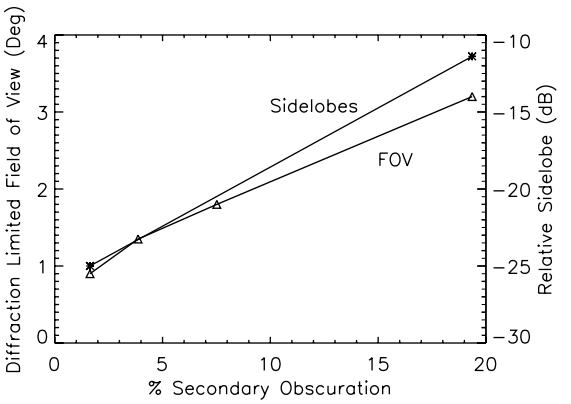

Fig. 1. Grasp8 and Zemax simulations of a series of on-axis Ritchey–Cretian telescopes. All telescopes have the same aperture and $F/\#$. The diffraction limited FOV was determined by Zemax raytracing. The edge of the usable field was defined as where the Strehl ratio dropped to 0.8. The sidelobe level was determined by a Grasp8 simulation. The secondary obscuration is by area.

drives the Ritchey–Cretian design to a low-obscuration, high curvature, smaller FOV design. With the off-axis telescope, there is no such tradeoff.

4. Cross-polarization comparisons

Grasp8 was also used to compare the cross-polarization performance of the on- and off-axis designs. The cross-polarized beam was simulated for both a beam in the middle of the field, and for one at 1° away from the center. Fig. 2 shows one-dimensional cuts of the co- and cross-polar beams. From the left panel of Fig. 2, it is clear that for the center of the array, the cross-polar performance of the on-axis design is superior to the off-axis design, but the conclusion is quite different for the edge of the field. The right panel of Fig. 2 shows that the cross-polarization performance of the off-axis telescope is equivalent to the on-axis telescope for the edge of the field. Since most of the pixels in a uniform focal plane array are close to the edge, in terms of cross-polarization performance, there is no reason to prefer the on-axis design.

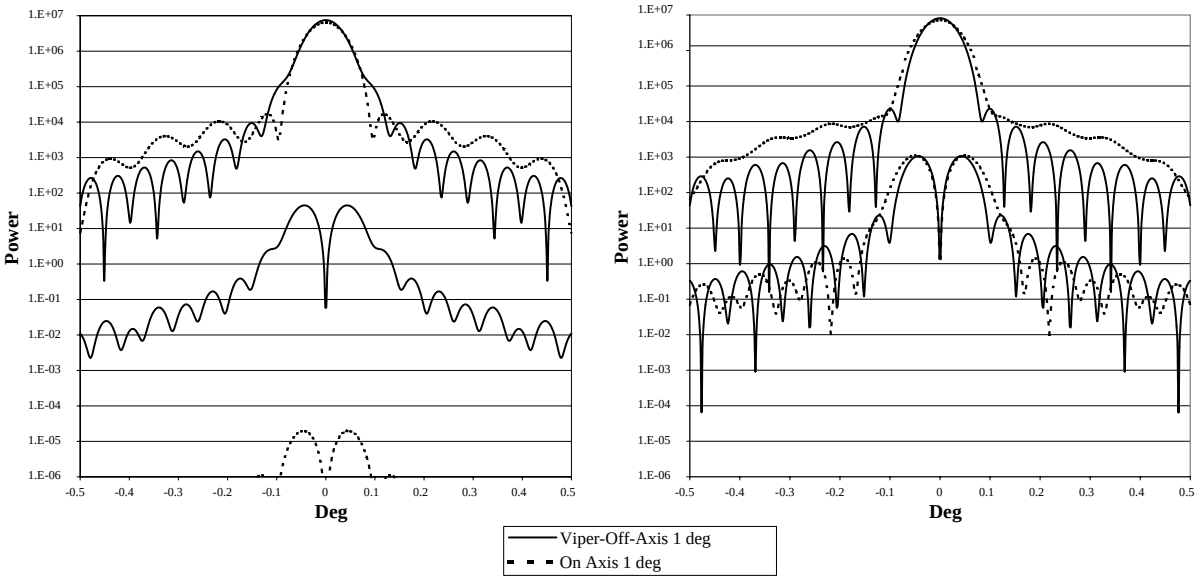

Fig. 2. Grasp8 beam simulations. The left panel is a simulation of the center of the field for both the on- and off-axis telescopes. A cut through both the co- and cross-polar beams is shown. The lower curves are the cross-polar beams. Cross-polar beams for an on-axis system have a classic four-lobe pattern, whereas for the off-axis telescope, the beams have a double-lobed pattern. Note that the cuts through the on-axis beams are artificially low because they were taken along a null of the beam. The right panel is a simulation of the beams for a pixel 1° away from the center of the array. The two lower curves are again the cross-polarized beams, and it is clear that both telescopes have similar performance.

5. Mizuguchi–Dragone condition

There are off-axis telescope designs that have better cross-polar performance than the Viper telescope. A tilt between the axis of secondary and primary of a pure Gregorian can cancel cross-polarization and astigmatism simultaneously (Mizuguchi et al., 1978; Dragone, 1982). A telescope that has this correction meets the Mizuguchi–Dragone condition. In addition to having low cross-polarization across the field, the diffraction-limited FOV of a Mizuguchi–Dragone telescope is better than an equivalent Ritchey–Cretian (Hanany and Marrone, 2002).

6. Instrumental-polarization correction

Since instrumental-polarization is induced by oblique reflections, off-axis telescopes have more than on-axis telescopes. It is, however, possible to correct for instrumental-polarization with a flat mirror. In an off-axis Mizuguchi–Dragone telescope, the primary and secondary are arranged in such a way that the tilts lie in the same plane, resulting in a net instrumental-polarization. A fold mirror that takes the rays out of the plane can be used cancel the effects of the first two mirrors. Fig. 3 is a diagram of how such a fold mirror would be implemented, and Fig. 4 shows the ex-

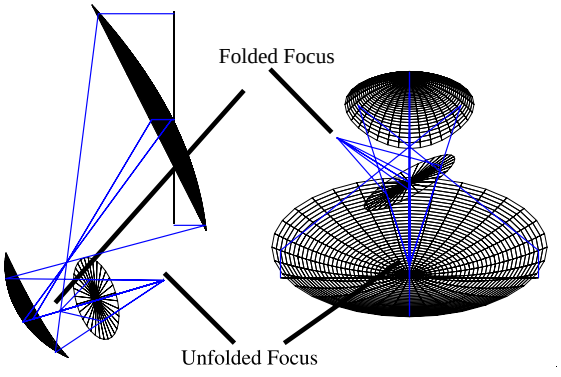

Fig. 3. Diagram of a instrumental-polarization correcting fold mirror. The left is the side view, and the right is a view from the top. The flat fold mirror takes the rays out of the plane of symmetry of the two main mirrors. The location of the Gregorian focus is shown both with and without the fold mirror.

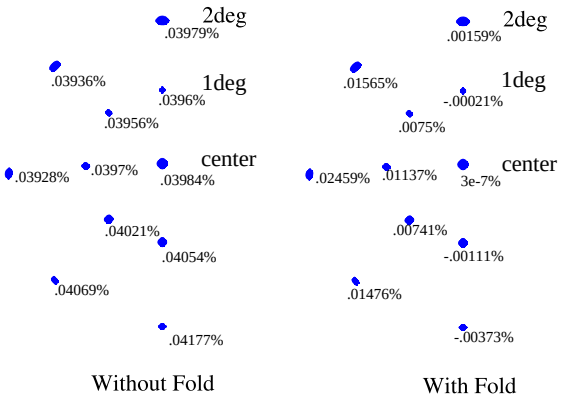

Fig. 4. Instrumental-polarization correction with the fold mirror. Two spot diagrams are shown for half of the field of the Viper telescope, both with and without the fold mirror. Since the fold mirror is flat, the spot diagrams themselves are identical. The instrumental-polarization of each field point was calculated using Zemax and inputting the finite conductivity of aluminum into the reflecting surfaces. Next to each field position is the net difference in power between vertical and horizontal polarizations, in other words, Q. It can be seen that for the center pixel, instrumental-polarization can be nulled. Furthermore, the induced Q is reduced across the rest of the field.

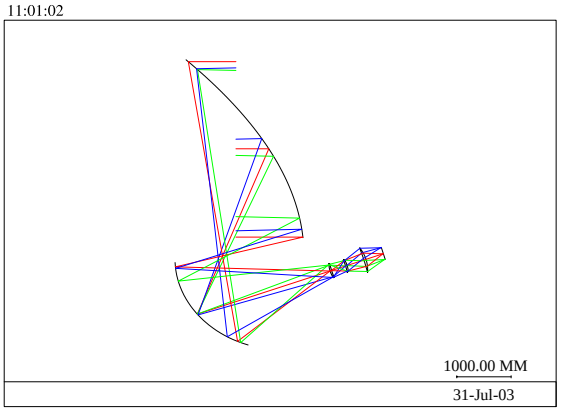

Fig. 5. Raytracing schematic of a full polarization-pure 3 m off-axis system. The field is diffraction limited across a 1.3° radius field, enough to support 1000 $2F/\#\lambda$ pixels. The main telescope is an offset Gregorian satisfying the Mizuguchi–Dragone condition. The reimaging optics are shown in detail in Fig. 6. The fold mirror from Fig. 3 is omitted for clarity. The aperture stop, located at the middle lens, is nominally imaged to the primary. Abberations at the extreme field rays produces a poor image of the Lyot on the primary, which is why the rays do not meet there. For field points closer to the middle of the field, the imaging of the Lyot is better.

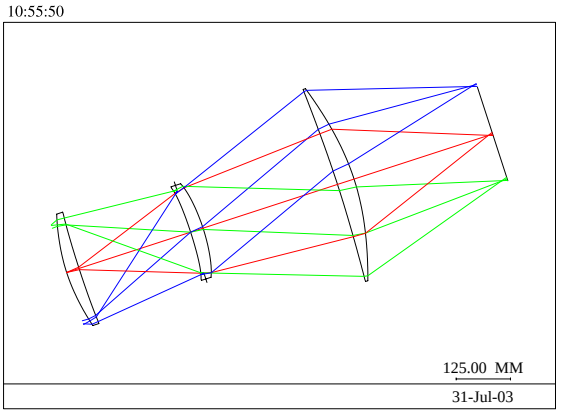

Fig. 6. Close-up view of the reimaging optics. All lenses have polynomial surfaces and are made of silicon. The first lens is a field lens, which images the Lyot stop, located at the second lens, onto the primary mirror. The second and third lenses are a collimating pair, used to reimage the field onto the array. Two lenses are used in an attempt to keep the diameter of both small. The second lens is at the Lyot stop, and it images the field to infinity. It was found that doing so helped to maintain a consistent $F/\#$ across the field. The last lens is positioned equidistant from the Lyot and the image plane, one focal length away from both. Keeping the Lyot one focal length away ensures that the system is telecentric. With so many surfaces, it is possible to keep the Strehl ratio above 0.95 for the entire 1000-$2F/\#\lambda$ element field.

tant to which instrumental-polarization can be mitigated across the array.

7. Reimaging optics

The use of large format arrays places additional constraints on optical systems, ones that are difficult to meet with a single pair of mirrors alone. With arrays that do not have well defined beam patterns from individual pixels, i.e. systems without corrugated feed horns, it is often necessary to use a cold aperture image, known as the Lyot stop, to block the sidelobes from the pixel. In bolemetric systems, the Lyot stop must be kept cold, requiring it to be small to fit inside a cryostat. Furthermore, the simplest schemes for fabricating large format arrays produce a device on wafers containing many elements. The wafers are flat, with the beams normal to the surface. This forces the image plane be both flat and telecentric.

The optical elements used to meet these constraints must do so without sacrificing the polarization purity of the front end optics. This can be done, for the center pixel at least, with the use of a cylindrically symmetric lens system. Fig. 5 is a raytracing diagram of a full optical system with reimaging optics, and Fig. 6 shows the reimaging optics alone. Explanations of both appear in the captions.

References

Dragone, C., 1982. IEEE Trans. Ant. Prop. 3, 331.

Hanany, S., Marrone, D.P., 2002. Comparison of designs of off-axis Gregorian telescopes for millimeter-wave large focal-plane arrays. Applied Optics 41, 4666–4670.

Heiles, C., Perillat, P., Nolan, M., Lorimer, D., Bhat, R., Ghosh, T., Howell, E., Lewis, M., O'Neil, K., Salter, C., Stanimirovic, S., 2001. All-Stokes parameterization of the main beam and first sidelobe for the arecibo radio telescope. PASP 113, 1247–1273.

Hu, W., Okamoto, T., 2002. Mass reconstruction with cosmic microwave background polarization. Astrophysical Journal 574, 566–574.

Johnson, B., 2003. E-mode Polarization Anisotropy of the CMBR with MAXIPOL, these proceedings.

Kesden, M., Cooray, A., Kamionkowski, M., 2003. Lensing reconstruction with CMB temperature and polarization. Physical Review D 67, 123507.

Knox, L., Song, Y., 2002. Limit on the detectability of the energy scale of inflation. Physical Review Letters 89, 11303.

Mizuguchi, Y., Akagawa, M., Yokoi, H., 1978. Electrical. Communications in Japan 61-B 3, 58.

O'Dell, C.W., 2001. A new upper limit on the angular scale polarization of the cosmic microwave background radiation. PhD thesis, University of Wisconsin – Madison, Department of Physics, Madison Wisconsin, astro-ph/0201224.